Desalination and Water Treatment
www.deswater.com

doi: 10.5004/dwt.2018.22651

127 (2018) 243–254
September

Removal of metronidazole from aqueous solutions by different natural surfactant-modified zeolitic tuffs

A. González-Ortiz[a,b], J.J. Ramírez-García[b], M.J. Solache-Ríos[a,*]

[a]Departamento de Química, Instituto Nacional de Investigaciones Nucleares (ININ), Carretera México-Toluca km. 36.5, Ocoyoacac, Estado de México, México, Tel. +52 5553297200 Ext: 12280; Fax: +52 5553297301; emails: marcos.solache@inin.gob.mx (M. Solache-Ríos), qfi.agonzalez@gmail.com (A. González-Ortiz)
[b]Laboratorio de Análisis Instrumental, Facultad de Química, Universidad Autónoma del Estado de México, Paseo Colón esquina Paseo Tollocan S/N, Colonia, Residencial Colón, Toluca, Estado de México, C.P. 50180, México, email: jjramirezg@uaemex.mx (J.J. Ramírez-García)

Received 23 November 2017; Accepted 21 June 2018

ABSTRACT

Metronidazole (MNZ) is an antiparasitic that has been found in wastewater. In this paper, the removal of MNZ by using modified zeolitic tuffs with two different surfactants (hexadecyltrimethylammonium bromide and benzyl hexadecyl dimethyl ammonium chloride) was studied. These modified materials were characterized by infrared spectroscopy, X-ray diffraction, scanning electron microscopy/energy dispersive X-ray spectroscopy and Brunauer–Emmett–Teller analysis. The cation exchange capacities and the points of zero charge were determined. The sorption kinetics show that the equilibrium times for all systems were similar about 15 h, the experimental data were best adjusted to the Ho–McKay model. The isotherms were linear indicating partition mechanism and the maximum adsorption capacity was in the order of 0.5 mg/g with an initial concentration of 20 mg/L of MNZ; the adsorption behavior of MNZ data at different temperatures was exothermic and the maximum adsorption capacity was observed between pH 5 and 6. The results show that the sorption efficiency depends on the origin of the zeolitic tuff and the surfactant used for the modification. These modified materials are effective to remove MNZ from aqueous solutions.

Keywords: Metronidazole; Sorption; Zeolitic tuff; Surfactants

---

1. Introduction

Water is essential for biological processes; the discharge of pollutants can deteriorate its quality and therefore the availability of safe water for human uses [1]. In recent years, the presence of traces of personal hygiene products and pharmacologically active chemical compounds in wastewater, surface water, and underground water has been detected; these chemicals are called emerging contaminants. Studies have demonstrated these compounds have toxic effects on aquatic organisms [2–4], they are persistent and their concentrations have been increasing. Metronidazole (MNZ) (Fig. 1) concentrations of 1.8–9.4 μg/L have been found in hospital effluents [5], this is an antibiotic and antiparasitic of the group of nitroimidazoles, effective to treat infectious diseases caused by anaerobic bacteria and protozoa and inhibits nucleic acid synthesis [6,7]. Human excretes from 6% to 18% of the doses in unchanged form when it is taken orally. It is also used in veterinary medicine as an antiparasitic, usually it is added to the food of farm animals such as poultry and fish; so, it accumulates in the tissues of such animals, in effluents of water from farms and fish farming industry [8,9]. The growth of soybean plants is affected by low concentrations of MNZ. The rhizosphere density of soil protozoa decreases 10 times with presence of 0.5 mg/g of MNZ [10]. Bendesky et al. [11] reported that

---

* Corresponding author.

1944-3994/1944-3986

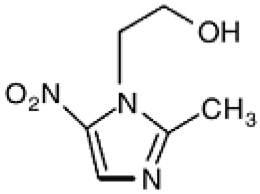

Fig. 1. Chemical structure of MNZ.

MNZ is an emerging contaminant that could be potentially carcinogenic and mutagenic because it is a proven mutagen in bacterial systems, genotoxic to human cells and carcinogenic to animals; however, the studies did not demonstrate that it is a risk factor for cancer in humans. According to the International Agency for Research on Cancer (IARC) [12], the evidence is sufficient to consider MTZ as an animal carcinogen, but insufficiently for humans. MNZ is not removed by conventional water treatments and its presence in water causes the development of antibiotic resistance bacteria [8,9].

The degradation of MNZ by nanoparticles of Fe^0 has been studied [8] and it has been removed from wastewater by commercial activated carbon and microorganisms [13]. Nolasco-Gómez et al. [14] studied the degradation of MNZ by an electrochemical method; they found 83.5% of degradation. Farzadkia et al. [7] applied the photocatalysis with TiO_2 nanoparticles, the removal efficiency was 99.48% at pH 7, but they did not identify the degradation products and sometimes these products have higher toxicity than the original compound; Ramavandi and Akbarzadeh [6] evaluated a coagulant extracted from *Plantago ovata* with $FeCl_3$ induced for the removal of MNZ, the disadvantages of this process was the generation of residual sludges; other material used for the same purpose is magnesium/aluminum layered double hydroxide nanoparticles [9].

Adsorption is an alternative method for the removal of these contaminants, it is a technology of low cost and the risk of generating of degradation products is low. In recent years, some materials such as red mud, fruit peel, clays, and zeolitic materials have been tested to remove emerging contaminants from water [15–17].

Zeolitic tuffs are crystalline aluminosilicates tetrahedral compounds; with exchangeable ions, such as Na^+, K^+, Ca^{2+}, and Mg^{2+} [18–20], they are environmentally and economical profitable [21], clinoptilolite type is one of the most abundant natural material [21]; the general formula of clinoptilolite is $(Ca, Na_2, K_2)_3[Al_6Si_{30}O_{72}]\cdot 24H_2O$ [18,21]. Several authors have proposed the modification of the zeolitic tuffs surfaces with cationic surfactants such as cetyl-pyridinium chloride (CPC), octadecyl dimethyl benzyl ammonium chloride (ODMBA), hexadecyltrimethylammonium bromide (HDTMA), and benzyl hexadecyl dimethyl ammonium chloride (BCDMA), in order to make their surfaces hydrophobic, [19,20,22–26]. Sorption studies on the removal of organic molecules using surfactant-modified zeolitic tuffs have been reported. Benzene, toluene, ethylbenzene, *p*-xylene, and *o*-xylene adsorption from aqueous solutions using HDTMA-modified zeolite Y was reported and efficiencies from 77% to 92% were found [27]; ODMBA-modified bentonite was used to remove aspirin and atenolol and the efficiencies were 80% and 86%, respectively [26]; CPC-modified clinoptilolite was used to remove diclofenac, it was observed that the adsorption increased as the surfactant concentration increased on the surface of clay [25]. The removal of MNZ has not been reported using surfactant-modified zeolitic tuffs to the best of our knowledge, however, this method promises to be efficient, safe, and economical for the removal of pharmaceuticals from water. Therefore, the aim of this work was to determine the adsorption behavior of MNZ from aqueous solution by surfactant-modified zeolitic tuffs, considering two zeolitic tuffs from different origin and two surfactants (HDTMA and BCDMA).

2. Experimental

2.1. Chemicals

The zeolitic tuffs type clinoptilolite used in this work were from the States of San Luis Potosí (ZeS) and Oaxaca (ZeO), Mexico. The samples were ground in an agate mortar and sieved to obtain three different particle sizes (10–20, 20–30, and 30–40 mesh).

2.2. Methods

2.2.1. Analytical method

MNZ concentration was measured by high-performance liquid chromatography (HPLC). The measurements parameters, namely suitability, accuracy, linearity, limit of detection, and quantification were determined. These parameters accomplished the national and international specifications.

2.2.2. Modification of zeolitic tuffs with sodium chloride

Samples of 100 g of natural zeolitic tuffs were refluxed with 1,000 mL of a 0.1 M NaCl solution for 3 h, then the phases were separated, this process was done twice, finally zeolitic tuffs were washed with deionized water until chloride ions were not found in the solution by the test with $AgNO_3$, labeled as ZeONa and ZeSNa.

2.2.3. Effective cation exchange capacity

100 mg of sodium zeolitic tuff were left in contact with 10 mL of 0.1 M CH_3COONH_4 solution, at 293 K and 120 rpm for 72 h. The supernatant was decanted, and sodium was determined by atomic absorption spectroscopy [28,29].

2.2.4. Modification of the zeolitic tuffs with the surfactants

Samples of 100 g of ZeONa were left in contact with 100 mL of 10 mmol/L BCDMA-Cl (B) or HDTMA-Br (H) solutions at 303 K for 72 h and 120 rpm (ZeOB and ZeOH, respectively). The same procedure was performed with ZeSNa using 20 mmol/L of the surfactants (ZeSB and ZeSH, respectively). The solids were washed with distilled water and then dried at room temperature.

2.2.5. Internal cation exchange capacity

100 mg of each material: Zeolitic tuff from Oaxaca modified with HDTMA (ZeOH) or BCDMA (ZeOB); zeolitic

tuff from San Luis Potosí modified with HDTMA (ZeSH) or BCDMA (ZeSB) were left in contact with 10 mL of 0.1 M CH_3COONH_4 solution, at 293 K and 120 rpm for 72 h. The amount of sodium exchange in the remaining solutions was analyzed by atomic absorption spectroscopy.

2.2.6. Point of zero charge (pH_{PZC})

100 mg of each zeolitic tuff samples were left in contact with 10 mL of a 0.1 M $NaNO_3$ solution of different pH, which were previously adjusted from 1 to 11 (pH_i) with intervals of one unit; by adding 0.1 M HCl or NaOH solutions. The samples were shaken at 293 K for 72 h and 120 rpm. Then the samples were decanted and the final pH (pH_f) of each solution was measured.

2.2.7. Scanning electron microscopy and Elemental analysis (EDS)

The samples were supported on a copper tape. The analysis was carried out by using a JEOL scanning electron microscopy (SEM), model JSM 5900LV, with an acceleration voltage of 20 kV. In all cases, the images were obtained with a backscattered electron detector. Energy dispersive X-ray spectroscopy (EDS) analysis was performed by using a PentaFetx Oxford model 7274.

2.2.8. X-ray diffraction

Analyses were performed by using an X-ray diffractometer mark Siemens model D5000 with a copper anode λ = 1.5418 Å, Kα radiation was selected diffracted beam monochromator, the range 2θ was 5°–80°. The diffractograms were compared with the diffraction patterns with the Joint Committee on Powder Diffraction Standards (JCPDS).

2.2.9. Characterization by infrared spectroscopy

Infrared (IR) spectra were obtained between 4,000 and 400 cm^{-1} by using spectrophotometer Nicolet ESP 360 FT-IR. The samples were prepared using KBr-zeolitic tuff ratio of 95:5.

2.2.10. Specific surface area (Brunauer–Emmett–Teller)

Isotherms were determined by standard multipoint nitrogen adsorption techniques, by using a Belsorp Max by BEL Japan INC. Zeolitic tuffs samples were heated at 453 K for 3 h before the analysis.

2.2.11. Effect of pH on the sorption of MNZ

100 mg of each surface-modified zeolitic tuff (ZeOH, ZeOB, ZeSH, and ZeSB) were left in contact with 10 mL of MNZ (20 mg/L) of different pH. The pH of solutions were previously adjusted from 1 to 11 of pH with intervals of one unit, using 0.1 M HCl or NaOH solutions and the mixtures were stirred for 72 h at 293 K and 120 rpm. The pH was measured by using a pH meter mark PHM210 and MNZ was analyzed by HPLC in the remaining solutions.

2.2.12. Sorption kinetics

100 mg of each surfactant-modified zeolitic tuff (ZeOH, ZeOB, ZeSH, and ZeSB) and 10 mL of MNZ (20 mg/L) were stirred at different times (0.25, 0.5, 1, 2, 4, 6, 7.5, 15, 18, 24, 48, and 72 h) at 293 K and 120 rpm. The initial concentration of the MNZ solutions were 20 mg/L because the validation of the analytical method by HPLC showed a good linearity and the limits of quantification were 0.03 mg/L; therefore, if the adsorption were up to 99.85%, it could be quantified accurately. It is important to note that the unmodified zeolitic tuffs did not adsorb any quantity of MNZ.

MNZ was analyzed in the remaining solutions by using a HPLC mark Waters®, model 1515 dual UV detector. The mobile phase consisted in methanol:water (20:80). The chromatographic separations were carried out under isocratic elution. The flow rate was 1 mL/min, the column used was a Bondapack C18 4.6 × 300 mm, particle size of 5 µm, the injection volume was 20 µL, and wavelength was set at 320 nm.

All experiment were performed in duplicate. The amount of MNZ adsorbed q_t (mg/g) was calculated by the following equation:

$$q_t = \frac{\left(C_0 - C_t\right)}{W} \times V \tag{1}$$

where C_o (mg/L) is the initial concentration of MNZ, C_t (mg/L) is the concentration at time (t), V (L) is the volume of drug solution, and W (g) is the mass of surface modified zeolitic tuff used. It is important to note that the initial pH values in the experiments were from 5.0 to 5.2 and the equilibrium values between 5.2 and 5.4.

2.2.13. Isotherms

100 mg of each surfactant-modified zeolitic tuff (ZeOH, ZeOB, ZeSH, and ZeSB) were placed in contact with 10 mL of MNZ of different concentrations (0.5, 1.0, 2.0, 5.0, 8.0, 10.0, 12.0, 15.0, 17.5, and 20 mg/L). The mixtures were stirred for 72 h at 293, 303, and 313 K and 120 rpm. These experimental conditions were selected for comparison purposes because these conditions were used elsewhere [30,31]. 10 mL of each MNZ solution was used, because it is an adequate volume to carry out the quantification of MNZ in duplicate. The samples were decanted and analyzed as described above.

3. Results and discussion

3.1. Analytical method

The measurements parameters were determined, and they were in the range of accepted values by national and international specifications [32–35], Table 1.

3.2. Effective cation exchange capacity

The effective cation exchange capacities (EfCECs) of both zeolitic tuffs (ZeO and ZeS) of three different particle sizes (between 10–20, 20–30, and 30–40 mesh) were determined. Sodium cations of the zeolitic tuffs were exchanged by ammonium ions and the amounts of sodium were analyzed. The results show the amounts of Na^+ exchanged

Table 1
Parameters for MNZ measurements by HPLC

Parameter	Experimental values	Accepted values [26–29]
Suitability	%CV = 1.40	%CV ≤ 2
	K' = 2.15	K' ≥ 2.00
	T = 1.34	T ≤ 2.00
	N = 8,741	N ≥ 2,000
System accuracy	%CV = 1.03	%CV ≤ 1.50
Linearity	R^2 = 0.998 with 10 points	R^2 ≥ 0.980 with minimum 5 points
Accuracy of the method	%CV = 1.27	%CV ≤ 2 from 2 analysts in 2 different days
Accuracy	%CV = 1.21 (recovery)	%CV of recovery ≤ 2.00
	CI (μ) = 98.29%–101.03%	CI (μ) = 98.0%–102.0%
Limit of detection and quantification	DL = 0.03 mg/L	Determined by the signal-to-noise method[a]
	QL = 0.10 mg/L	

CV is the coefficient of variation between each injection of the samples.
K′ is the capacity factor which indicates the rate of migration of the solute through the stationary phase.
T is the tailing factor that indicates the asymmetry of the peaks.
N is the theoretical plates of the column.
CI is the confidence interval.
DL is the detection limit and QL is the limit of quantification.
[a] The signal-noise method consists in obtaining an analytical signal three times higher than background for DL and 10 times for the QL.

were similar for the samples of different particle sizes of each zeolitic tuff; the EfCEC of ZeO is higher than ZeS. The samples of 20–30 mesh were selected to perform the experiments, because this size is the intermediate and the results are shown in Table 2. These results agree with those reported by Leyva-Ramos et al. [28] on the EfCEC of ZeS and they did not find any significant difference as well in samples of different particle sizes.

Yanev et al. [36] reported that the content of clinoptilolite in this zeolitic tuff was 49%–52%. The EfCEC is proportional to the amount of clinoptilolite in the tuffs, the EfCEC for ZeS is a half of the value for ZeO, and thus the percentage of clinoptilolite in this last sample is much lower, the percentage of clinoptilolite in this tuff has not been determined.

3.2.1. Internal cation exchange capacities

Table 3 shows the internal cation exchange capacities (ICECs) of the sodium-modified zeolitic tuffs determined by using both surfactants HDTMA and BCMA. The difference between the EfCEC and ICEC is the external cation exchange capacity (ECEC). The functionalization of natural zeolitic tuffs with cationic surfactants allows changing the hydrophilic to hydrophobic properties on the surface of these materials. It has been reported that the counterion influences the maximum sorption of HDTMA on clinoptilolite-rich tuff and it has been demonstrated that HDTMA-Br forms bilayer more than Cl^- on this kind of tuffs [29,37,38]. The ECEC represents only the exchange sites on the surface of the zeolitic tuffs, this is approximately 3% of EfCEC of both zeolitic tuffs

Table 2
Effective cation exchange capacities of natural and sodium zeolitic tuffs

Sieve	ZeO (meq/g of Na^+)	ZeONa (meq/g of Na^+)	ZeS (meq/g of Na^+)	ZeSNa (meq/g of Na^+)
10–20	0.888 ± 0.001	0.908 ± 0.090	0.181 ± 0.001	0.511 ± 0.037
20–30	0.937 ± 0.040	0.945 ± 0.020	0.172 ± 0.010	0.491 ± 0.027
30–40	0.901 ± 0.007	0.987 ± 0.046	0.180 ± 0.011	0.505 ± 0.024

Table 3
Internal and external cation exchange capacities of modified surface zeolitic tuffs

Zeolitic Tuff	EfCEC	Surfactant	ICEC (meq/g of Na^+)	ECEC (meq/g of Na^+)
ZeONa	0.945	HDTMA	0.914	0.031
ZeONa		BCDMA	0.921	0.024
ZeSNa	0.491	HDTMA	0.456	0.035
ZeSNa		BCDMA	0.475	0.016

and 97% is the internal EfCEC. Salinas et al. [39] reported an ECEC of 0.01 meq/g determined by HDTMA and the ICEC of 0.63 meq/g. Leyva-Ramos et al. [28] reported an ECEC of 0.3 meq/g and an EfCEC of 1.3 meq/g for a zeolitic tuff from San Luis Potosí.

3.3. Scanning electron microscopy

Fig. 2 shows the SEM images of natural- and sodium-modified zeolitic tuffs, typical morphology of clinoptilolite of coffin and cubic-like crystals are observed [40]. SEM images of ZeO and ZeS show that structures were not modified by the treatment with NaCl solutions.

Fig. 3 shows the images of ZeOH, ZeOB, ZeSH, and ZeSB, typical clinoptilolite crystals are observed and are similar to the natural- and sodium-modified tuffs. The main elements found by SEM/EDS in the zeolitic tuffs were Si, Al, and O; ZeO has a higher amount of sodium than ZeS and the percentages of ions such as K^+, Ca^{2+}, and Mg^{2+} decreased in both zeolitic tuffs after modifications with sodium chloride solutions. Carbon and nitrogen were found in ZeOH, ZeOB, ZeSH, and ZeSB; indicating the presence of the surfactants in the zeolitic tuffs, these elements were not found in natural and sodium zeolitic tuffs (Table 4). These results are similar to those reported by Díaz-Nava et al. [41] and Gamboa et al. [30].

3.4. X-ray diffraction

Fig. 4 shows the diffractograms of ZeO, ZeOH, and ZeOB. Clinoptilolite (JCPDS 01-085-1797), muscovite (JCPDS 01-085-1855), and mordenite (JCPDS 00-049-0924) were found in all materials. The diffractograms were similar after modifications.

Clinoptilolite (JCPDS 01-085-1797), quartz (JCPDS 01-086-1565), and muscovite (JCPDS 01-085-1855) were found in the natural- and surfactant-modified zeolitic tuff (ZeS) (Fig. 5); the diffractograms were similar after modifications. Quartz and other phases like muscovite and mordenite have been reported as common impurities of zeolitic tuffs [42].

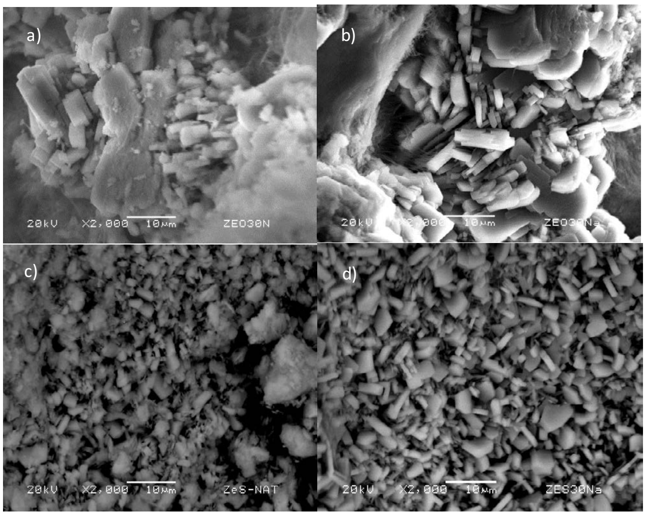

Fig. 2. SEM images of natural zeolitic tuff from Oaxaca, Mexico (a); sodium zeolitic tuff from Oaxaca (b); natural zeolitic tuff from San Luis Potosí (c); and sodium zeolitic tuff from San Luis Potosí (d).

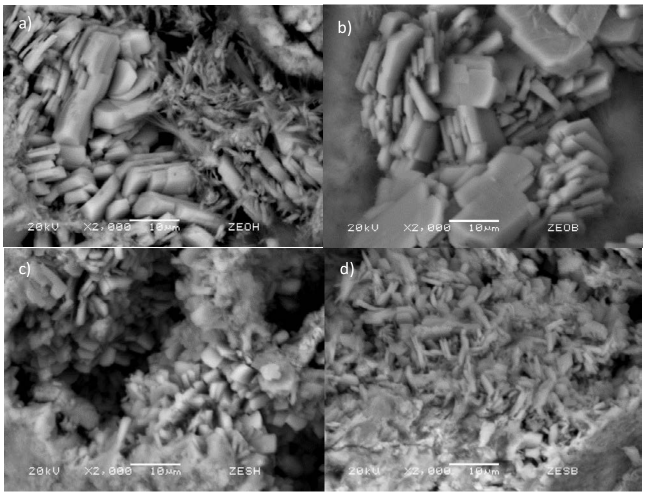

Fig. 3. SEM images zeolitic tuff from Oaxaca modified with HDTMA (a); zeolitic tuff from Oaxaca modified BCDMA (b); zeolitic tuff from San Luis Potosí modified with HDTMA (c); and zeolitic from San Luis Potosí modified with BCDMA (d).

Table 4
Elementary chemical compositions of the natural, sodium, and surfactants-modified zeolitic tuffs

Element	ZeO (%)	ZeONa (%)	ZeOH (%)	ZeOB (%)	ZeS (%)	ZeSNa (%)	ZeSH (%)	ZeSB (%)
Na	3.06 ± 0.34	3.66 ± 0.20	2.47 ± 0.23	2.25 ± 0.21	0.54 ± 0.11	2.04 ± 0.18	1.24 ± 0.10	1.33 ± 0.01
Mg	0.15 ± 0.05	0.13 ± 0.10	–	–	0.17 ± 0.06	0.23 ± 0.08	–	–
Ca	0.73 ± 0.13	0.85 ± 0.10	0.44 ± 0.08	0.56 ± 0.18	3.55 ± 0.65	2.96 ± 0.21	1.67 ± 0.26	1.46 ± 0.28
K	2.27 ± 0.35	1.75 ± 0.34	1.23 ± 0.56	1.28 ± 0.21	2.14 ± 0.50	2.57 ± 0.49	1.21 ± 0.23	1.41 ± 0.23
Si	41.70 ± 1.66	41.07 ± 0.87	28.50 ± 0.70	26.77 ± 3.46	41.28 ± 1.17	42.97 ± 0.73	27.99 ± 2.25	26.96 ± 3.01
Al	7.61 ± 0.49	7.26 ± 0.28	5.20 ± 0.17	5.17 ± 0.21	7.41 ± 0.85	7.88 ± 0.35	5.30 ± 0.46	5.32 ± 0.49
Fe	1.41 ± 0.43	0.95 ± 0.21	0.86 ± 0.31	0.93 ± 0.18	1.38 ± 0.63	2.30 ± 1.23	1.09 ± 0.29	1.06 ± 0.25
O	44.05 ± 1.40	44.32 ± 0.74	42.71 ± 0.62	40.70 ± 2.06	44.52 ± 2.17	41.43 ± 1.78	41.56 ± 1.57	40.01 ± 1.41
C	–	–	12.32 ± 0.32	15.01 ± 4.29	–	–	12.77 ± 1.83	15.47 ± 3.20
N	–	–	6.27 ± 0.36	7.32 ± 1.45	–	–	7.16 ± 0.77	6.97 ± 0.98

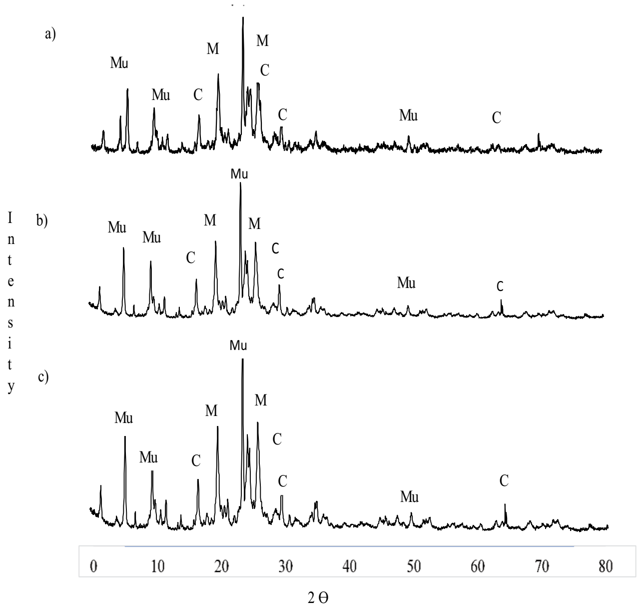

Fig. 4. XRD diffractograms of (a) ZeO, (b) ZeOH, and (c) ZeOB compared with the JCPDS (M = Mordenite; Mu = Muscovite; C = Clinoptilolite).

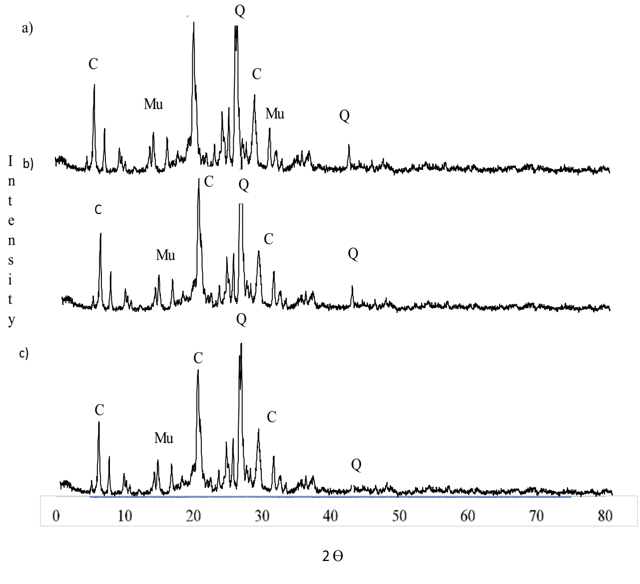

Fig. 5. XRD of (a) ZeS, (b) ZeSH, and (c) ZeSB compared with the JCPDS (Q = Quartz; Mu = Muscovite; C = Clinoptilolite).

3.5. Point of zero charge (pH_{PZC})

The points of zero charge of the natural and modified zeolitic tuffs are presented in Table 5. The pH_{PZC} values slightly increased after the materials were modified with the surfactants, these results agree with those reported by Gamboa et al. [30]; they reported the pH_{PZC} of a zeolitic tuff from Puebla, Mexico modified with HDTMA, the pH_{PZC} values reported were 7.0, 8.1, and 8.6 for the natural zeolitic tuff and surfactant-modified zeolitic tuff with 0.25 and 0.50 mmol/g solutions, respectively.

Table 5
Point of zero charge of the zeolitic tuffs

Material	Point of zero charge (pH)
ZeO	5.84 ± 0.19
ZeONa	6.05 ± 0.09
ZeOH	6.65 ± 0.12
ZeOB	6.84 ± 0.09
ZeS	6.21 ± 0.18
ZeSNa	6.35 ± 0.10
ZeSH	6.88 ± 0.09
ZeSB	7.11 ± 0.03

3.6. IR spectroscopy

Fig. 6 shows the IR spectra of zeolitic tuffs (ZeO, ZeOH, and ZeOB). Bands at 3,614 cm^{-1} are related to acidic hydroxyls Si–O(H)–Al and at 3,605 cm^{-1} attributed to the vibration of the hydrogen-bonding hydroxyl groups, characteristic of the clinoptilolite [31]. The band at 1,631 cm^{-1} is attributed to the absorbed water [43]. The bands at 1,214 and 1,041 cm^{-1} are related to O-Si-O. The peaks at 738–524 and 674–458 cm^{-1} are associated to free tetrahedral group SiO_4. ZeOH and ZeOB presented vibrations at 2,935–2,919 cm^{-1} and between 2,869 and 2,867 cm^{-1}, these bands are attributed to CH_2, which confirm the surfactants modifications of the zeolitic tuffs.

Fig. 7 shows the IR spectra of ZeS, ZeSH, and ZeSB, these spectra are similar to those of ZeO. The sorption of HDTMA occurs only on the surface of zeolitic tuffs because of the sizes of the molecule of HDTMA and the channels of the zeolitic tuffs, the bands attributed to the internal Si–O(Si) and Si–O(Al) vibrations in tetrahedral, aluminum- and silicon-oxygen in the range of 1,200–400 cm^{-1} remain unchanged [22,31,44].

3.7. Specific surface areas (Brunauer–Emmett–Teller)

Table 6 shows that the surface areas decreased after the zeolitic tuffs were modified with the surfactants, because the surfactants are located on the surfaces of the zeolitic tuffs and the pores may be clogged. A similar behavior has been observed elsewhere [30,31].

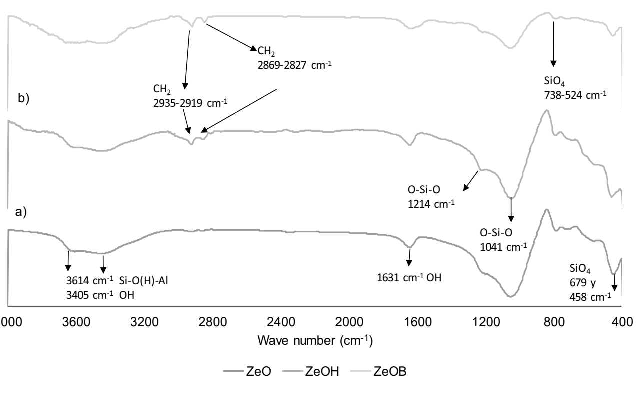

Fig. 6. IR Spectra of (a) ZeO, (b) ZeOH, and (c) ZeOB.

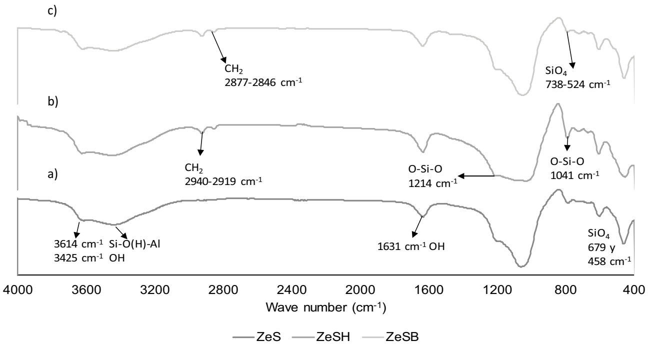

Fig. 7. IR Spectra of (a) ZeS, (b) ZeSH, and (c) ZeSB.

Table 6
Specific surface areas of natural and surfactant modified zeolitic tuffs

Zeolitic tuff	ZeO	ZeOH	ZeOB	ZeS	ZeSH	ZeSB
Pore volume (cm^3/g)	0.079	0.045	0.041	0.165	0.142	0.133
Surface area (m^2/g)	52.690	28.355	25.101	25.475	13.879	14.657
Pore diameter (nm)	60.644	63.613	65.486	36.009	40.981	36.396

3.8. Effect of pH on the sorption of MNZ

The chemical species distribution diagram of MNZ (Fig. 8) at different pH values was determined considering the pK_a's reported by Noori-Sepehr et al. [9] (2.58 and 14.48), below the first pK_a value the predominant species are positive charged and between 2.58 and 14.48 the predominant species of MNZ are neutral; in this last interval the highest adsorption was observed. The adsorption of MNZ increased as the pH increased up to pH 5 and a plateau was observed between pH 5 and 6 and then the adsorption decreased (Fig. 9). The point of zero charge of the modified surfaces zeolitic tuffs were 6.8 ± 0.4; then it can be said that below this pH value, the materials are positively charged and at higher pH values are negatively charged. Noori-Sepehr et al. [9] studied the effect of pH on the sorption of MNZ by magnesium/aluminum layered double hydroxide nanoparticles; they obtain an increase in the sorption of MNZ from pH 3 up to 9.

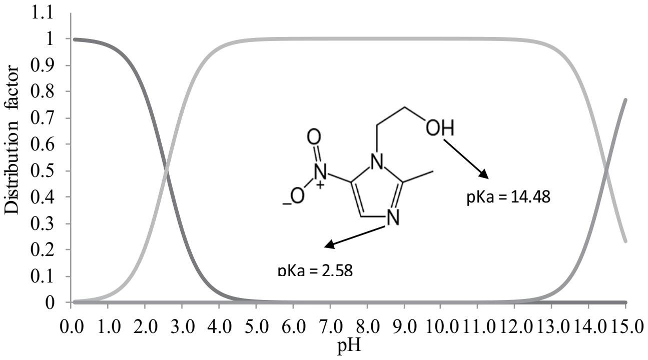

Fig. 8. Distribution diagram of MNZ chemical species.

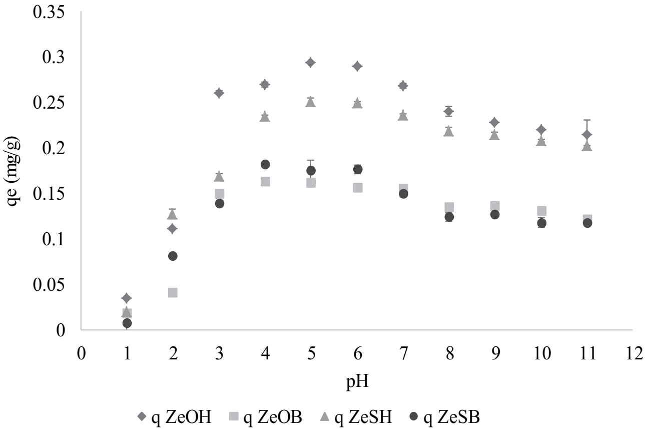

Fig. 9. pH effect of MNZ sorption.

3.9. Sorption kinetics

The sorption kinetics behaviors give information about the equilibrium time, the adsorption rate, and the possible mechanisms involved. Different kinetic models have been reported in the literature, the experimental results were fitted to nonlinear equations of the Lagergren, Elovich, and Ho models using Origin version 8.1 software:

3.9.1. Kinetic models

The equation of Lagergren model (Eq. (2)) considers physical sorption, homogenous sorbents and that the rate is proportional to the solute concentration [45].

$$q_t = q_e\left(1 - e^{-K_L t}\right) \tag{2}$$

where q_e (mg/g) is the amount of adsorbed MNZ in the equilibrium, K_L (h^{-1}) is the sorption constant of Lagergren, and t (h) is contact time.

Elovich model describes chemisorption mechanism on highly heterogeneous materials [45]. The equation of the model is as follows:

$$q_t = \beta \ln(\alpha\beta) + \beta \ln(t) \tag{3}$$

where α (mg/g h) is the initial sorption rate and β is the desorption constant (mg/g).

The model proposed by Ho and McKay [46] establishes that the rate limiting step implicates valence forces through the sharing or exchange of electrons between solute and adsorbent; therefore, it assumes that the process is chemisorption, the equation of the nonlinear model is the following:

$$q_t = \frac{q_e K_H t}{1 + q_e K_H t} \tag{4}$$

where K_H (g/mg h) is the sorption constant rate of Ho–McKay model and t (h) is the time.

Fig. 10 shows the sorption kinetic behavior of MNZ by ZeOH, ZeOB, ZeSH, and ZeSB, the adsorption rates were high at the beginning of the sorption processes and the equilibriums were reached in about 15 h for all systems. The parameters of the sorption of MNZ calculated from the experimental data and models are shown in Table 7.

The model of Lagergren has been related to physisorption mechanism and the other two models to chemisorption. The sorption kinetics behaviors are similar for all materials (ZeOH, ZeOB, ZeSH, and ZeSB). The experimental data were best adjusted to the Ho–McKay model (Fig. 10); because the R^2 values were the highest and the differences between the experimental and calculated q_e values are lower for this model in comparison with the Lagergren model (Table 7). The constant α shows the initial sorption rates were higher for ZeO than ZeS; this could be because the first has a higher adsorption capacity than the second one. The β constant is related to desorption, which was higher for ZeO than ZeS; this behavior indicates MNZ binds weaker to ZeO than ZeS, this property could be useful when regeneration of the saturated material is required. The sorption constant rates of Ho are higher for the surfactant modifies zeolitic tuffs from Oaxaca than San Luis Potosí, the quantity of sodium in these materials could be responsible for these behaviors, and the zeolitic tuff of Oaxaca contains more sodium than the material from San Luis Potosí.

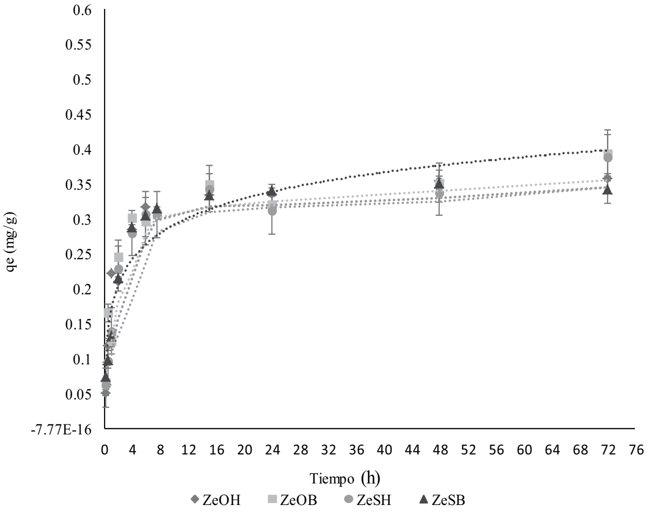

Fig. 10. Sorption kinetics of MNZ by ZeOH, ZeOB, ZeSH, and ZeOB, the lines correspond to the adjustments of experimental data to the Ho model.

It has been studied the sorption of MNZ with magnesium/aluminum layered double hydroxide nanoparticles, which have hexagonal forms with diameter between 200 and 1,000 nm and they obtain a q_e = 3.382 mg/g from aqueous solution with an initial concentration of 10 mg/L and contact time of 120 min [8]. In another work, it was found that the Fe-modified sepiolite showed a q_e = 2.737 mg/g, the experimental data were fitted to the pseudo-second-order kinetic model, and the isotherms were best adjusted to Freundlich model [47]. Liu et al. [48] reported the sorption of MNZ with active carbon, they obtained a q_e = 0.615 mg/g from aqueous solution with an initial concentration of 5 mg/L and Won Seo et al. [5] obtained a q_e = 90.8 mg/g with active carbons and with metal-organic frameworks functionalized with urea a q_e = 188 mg/g. Sun et al. [49] studied the sorption of MNZ onto biochar derivate from sugarcane bagasse, they reported a q_e experimental value of 4.393 mg/g using an initial concentration of 20 mg/L. Manjunath et al. [50] used a powder active carbon and concrete containing graphene, they obtained maximum MNZ concentration capacities between 25–32.8 mg/L and 0.041–0.002 mg/g, respectively, using initials concentrations of MNZ between 5 and 100 mg/L. Kalhori et al. [51] found the maximum adsorption capacity of the light weight expanded clay aggregate surface (LECA) of 56.31 mg/g and for LECA coating with MgO nanoparticles 84.55 mg/g. Noori-Sepehr et al. [9] reported a q_e of 24 mg/g using biochar and an initial concentration of 40 mg/L and when the initial concentration was 20 mg/L, a q_e of 10.667 mg/L was found.

3.10. Sorption isotherms

The adsorption isotherms of MNZ at 293, 303, and 313 K by ZeOH, ZeOB, ZeSH, and ZeSB were linear and are shown in Figs. 11–14. The adsorption behavior of MNZ by all materials was similar between 293 and 313 K.

Table 8 shows the slopes of each isotherm; the slopes values decrease as the temperature increases. The maximum

Table 7
Kinetic parameters of the adsorption of MNZ by ZeOH, ZeOB, ZeSH, and ZeSB

Model	ZeOH	ZeOB	ZeSH	ZeSB
Lagergren	K = 0.123 (h^{-1}) q_e = 0.011 mg/g R^2 = 0.920	K = 0.662 (h^{-1}) q_e = 0.336 mg/g R^2 = 0.869	K = 0.545 (h^{-1}) q_e = 0.334 mg/g R^2 = 0.950	K = 0.530 (h^{-1}) q_e = 0.334 mg/g R^2 = 0.976
Elovich	α = 1.668 (mg / g* h) β = 19.451 (mg/g) R^2 = 0.860	α = 1.509 (mg / g* h) β = 18.786 (mg/g) R^2 = 0.873	α = 0.983 (mg / g* h) β = 17.740 (mg/g) R^2 = 0.890	α = 1.123 (mg / g* h) β = 18.391(mg/g) R^2 = 0.872
Ho	K = 2.875 (g/mg h) q_e = 0.356 mg/g R^2 = 0.964	K = 2.519 (g/mg h) q_e = 0.364 mg/g R^2 = 0.920	K = 2.053 (g/mg h) q_e = 0.363 mg/g R^2 = 0.971	K = 2.098 (g/mg h) q_e = 0.361 mg/g R^2 = 0.986
q_{exp}	0.334 ± 0.019	0.353 ± 0.030	0.342 ± 0.007	0.344 ± 0.031

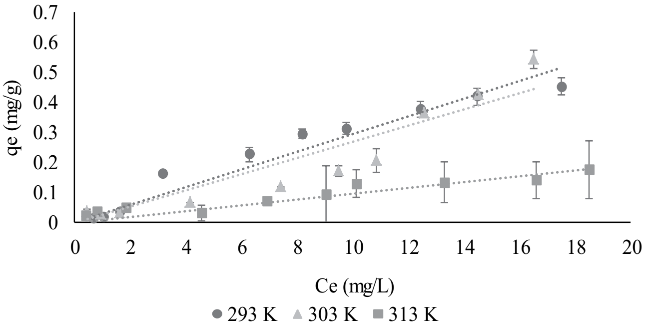

Fig. 11. Sorption isotherm of MNZ by ZeOH.

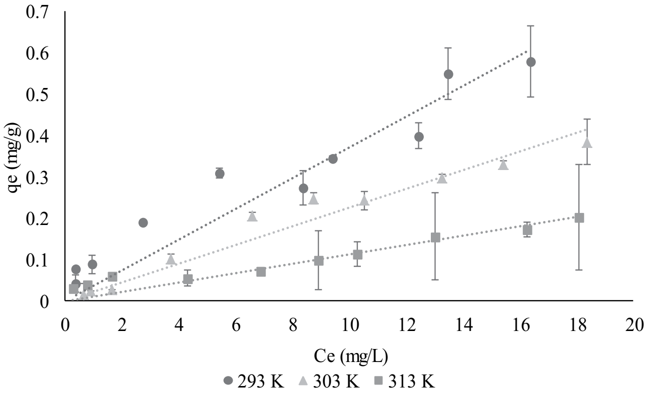

Fig. 12. Sorption isotherm of MNZ by ZeOB.

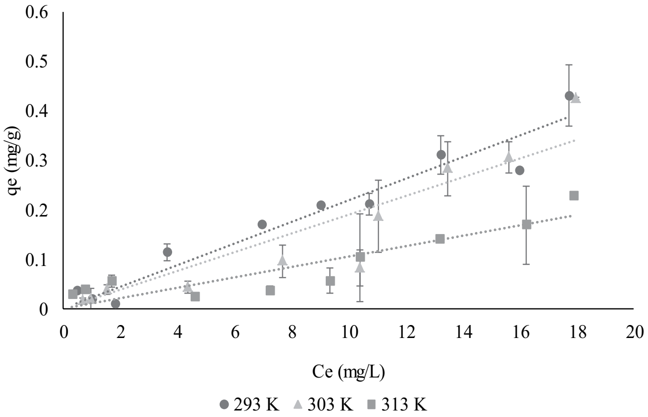

Fig. 13. Sorption isotherm of MNZ by ZeSH.

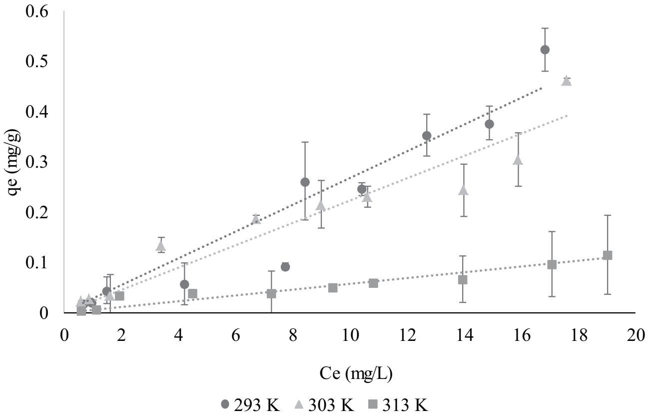

Fig. 14. Sorption isotherm of MNZ by ZeSB.

Table 8
Slopes (m) of the equations of the sorption isotherms (MNZ by ZeSH, ZeSB, ZeOH, and ZeOB)

Material	293 K	303 K	313 K
ZeOH	$Y = 0.029x$ $R^2 = 0.943$	$Y = 0.026x$ $R^2 = 0.884$	$Y = 0.009x$ $R^2 = 0.863$
ZeOB	$Y = 0.037x$ $R^2 = 0.890$	$Y = 0.022x$ $R^2 = 0.955$	$Y = 0.011x$ $R^2 = 0.881$
ZeSH	$Y = 0.021x$ $R^2 = 0.936$	$Y = 0.019x$ $R^2 = 0.860$	$Y = 0.010x$ $R^2 = 0.802$
ZeSB	$Y = 0.026x$ $R^2 = 0.913$	$Y = 0.022x$ $R^2 = 0.902$	$Y = 0.005x$ $R^2 = 0.926$

Table 9
Maximum adsorption of MNZ with initial concentration of 20 mg/L by modified surfaces zeolitic tuffs

Material	293 K	303 K	313 K
	q_e (mg/g)	q_e (mg/g)	q_e (mg/g)
ZeOH	0.542 ± 0.02	0.452 ± 0.03	0.202 ± 0.12
ZeOB	0.580 ± 0.09	0.461 ± 0.01	0.229 ± 0.01
ZeSH	0.431 ± 0.01	0.426 ± 0.06	0.175 ± 0.09
ZeSB	0.523 ± 0.04	0.385 ± 0.05	0.114 ± 0.07

adsorbed amounts of MNZ by the modified zeolitic tuffs are shown in Table 9. The adsorption of MNZ was highest at a temperature of 293 K, because the processes were exothermic. The modified zeolitic tuff from Oaxaca (ZeOH and ZeOB) adsorbed the highest amounts of MNZ; the higher cation exchange capacity of this tuff compared with the zeolitic tuff from San Luis Potosí could be responsible for this behavior.

Different authors have reported in similar adsorption systems that the mechanism that takes place in these conditions is partition, the solute is distributed between the organic and aqueous phases depending on the solubility of the solute, for example, Polesel et al. [52] reported that ciprofloxacin is distributed in the hydrophobic and aqueous phase of an activated sludge treated with $FeSO_4$ and KNO_3 under anaerobic conditions. HDTMA imparts hydrophobicity to zeolitic surfaces and has been used to remove chlorinated aliphatic compound and benzene derivatives, and both processes were described by the partition mechanism [52–54]. The sorption of phenol [55,56] and 4-chlorophenol [57] by a clinoptilolite-rich tuff modified with HDTMA were studied and the authors reported a partition mechanism. On the other hand, the sorption of the pharmaceuticals bisphenol A [24] and

17α-ethinylestradiol [31] by surfactant-modified zeolitic tuffs also showed a linear behavior.

3.11. Thermodynamic parameters

The $\Delta H°$ and $\Delta S°$ were calculated by using the van't Hoff equation as follows:

$$\ln K_c = \left(\frac{-\Delta H°}{R}\right)\left(\frac{1}{T}\right) + \frac{\Delta S°}{R} \quad (5)$$

and $\Delta G°$ by the following equation:

$$\Delta G° = \Delta H° - T\Delta S° \quad (6)$$

where T is the temperature in kelvin (K), R is the ideal gas constant (8.314 J/mol K), K_c is the equilibrium constant which indicates the ratio of the equilibrium concentration of the solute on the material to the concentration in solution, in this work the slopes (m) of the isotherms (Table 8) were used to calculate $\Delta H°$ and $\Delta S°$ instead of this parameter [58], Table 10 shows the equations obtained from the slopes (m) of the equations of the sorption isotherms versus $1/T$; $\Delta G°$ was evaluated at three different temperatures (293, 303, and 313 K); $\Delta H°$ and $\Delta S°$ were calculated from the slope and intercept of a plot of ln(m) versus $1/T$ [59]. Table 11 shows the thermodynamic parameters involved in the sorption of MNZ by ZeSH, ZeSB, ZeOH, and ZeOB.

The value of $\Delta H°$ is negative and indicates that the process is exothermic; thus, the adsorption of MNZ by the four modified surfaces zeolitic tuffs decreases with increasing the temperature. The value of $\Delta S°$ is negative indicating that the randomness decreases at their solid/solution interface and no significant changes occur in the internal structure of the modified surfaces zeolitic tuffs through the adsorption of MNZ; the values of $\Delta G°$ are positive, because the process is not spontaneous. These results agree with those reported by Noori-Sepehr et al. [9], they studied the sorption of MNZ by magnesium/aluminum layered double hydroxide nanoparticles and obtain values of $\Delta H°$ and $\Delta S°$ negatives and $\Delta G°$ positives, in an interval from 283 to 303 K.

Table 10
Equations of slopes (m) versus temperature (T)

Material	Equation	R^2
ZeOH	$\ln(m) = 5{,}052.0(1/T) - 20.611$	0.799
ZeOB	$\ln(m) = 5{,}491.4(1/T) - 21.994$	0.985
ZeSH	$\ln(m) = 3{,}346.3(1/T) - 15.164$	0.871
ZeSB	$\ln(m) = 6{,}996.7(1/T) - 27.293$	0.798

Table 11
Thermodynamic parameters of the sorption of MNZ by ZeSH, ZeSB, ZeOH, and ZeOB

Material	$\Delta H°$ (kJ/mol)	$\Delta S°$ (J/mol K)	$\Delta G°$ (kJ/mol)		
			293 K	303 K	313 K
ZeOH	–42.00	–171.36	8.20	9.91	11.63
ZeOB	–45.65	–182.86	7.92	9.74	11.57
ZeSH	–27.82	–126.07	9.11	10.37	11.63
ZeSB	–58.17	–226.91	8.31	10.58	12.85

4. Conclusions

The characterization of the zeolitic tuffs showed the ion exchange capacity of ZeO is higher than ZeS. There is not any significant difference between the cation exchange capacities of the zeolites with different particle sizes (10–20, 20–30, and 30–40 mesh). The diffractograms of X-ray diffraction (XRD) showed that there were not any important changes in the crystalline structure of ZeS and ZeO after modification with the HDTMA and BCDMA surfactants. The IR spectrum shows that there are not any changes in the structure of the aluminosilicates after modifications with NaCl and surfactants. The presence of HDTMA and BDHMA was evident because two bands appeared after modifications at 2,935–2,919 and 2,869–2,827 cm^{-1} corresponding to C–C and C–N bonds. However, the zeolitic tuffs did not present changes in the structure of coffin, typical of clinoptilolite. The pH$_{PZC}$ of the materials shows that there is not any significant difference between the modified surfaces zeolitic tuffs. The sorption kinetics of MNZ showed that there was not any significant difference between the adsorbed amounts and that the equilibrium times and the isotherms show a linear behavior indicating a partitioning mechanism. The adsorption capacity was in the order of 0.5 mg/g, using a 20 mg/L solution; however, the adsorption increases as the initial concentration of MNZ increases. The thermodynamic parameters show that the adsorption processes of all materials are exothermic and not spontaneous. The effect of pH showed that the neutral species have higher affinity for the adsorbent in pH ranges between 5 and 6. The results show the modified materials are effective to remove MNZ from aqueous solutions.

Acknowledgments

The authors acknowledge the financial support from CONACYT (Projects 215997) and CONACYT scholar grant no. 556031 for AGO.

References

[1] U. Ochuko, O. Thaddeus, O. Asuma, E. Ezo, A comparative assessment of Water Quality Index (WQI) and suitability of River Ase for domestic water supply in urban and rural communities in Southern Nigeria, Int. J. Hum. Soc. Sci., 4 (2014) 234–245.

[2] I. Akoteyon, A. Omotayo, O. Soladoye, O. Olaoye, Determination of Water Quality Index and suitability of urban river for municipal water supply in Lagos-Nigeria, Eur. J. Sci. Res., 54 (2011) 263–271.

[3] B.D. Blair, J.P. Crago, C.J. Hedman, R.D. Kappler, Pharmaceuticals and personal care products found in the Great Lakes above concentrations of environmental concern, Chemosphere, 93 (2013) 2116–2123.

[4] M. Gros, M. Petrovic, A. Ginebreda, D. Barceló, Removal of pharmaceuticals during wastewater treatment and environmental risk assessment using hazard indexes, Environ. Int., 36 (2010) 15–26.

[5] P. Won Seo, N. Abedin Khan, S. Hwa Jhung, Removal of nitroimidazole antibiotics from water by adsorption over metal–organic frameworks modified with urea or melamine, Chem. Eng. J., 315 (2015) 92–100.

[6] B. Ramavandi, S. Azbarzadeh, Removal of metronidazole antibiotic from contaminated water using a coagulant extracted from *Plantago ovata*, Desal. Wat. Treat., 55 (2015) 2221–2228.

[7] M. Farzadkia, E. Bazrafshan, A. Esrafili1, J. Yang, M. Shirzad-Siboni, Photocatalytic degradation of Metronidazole with illuminated TiO_2 nanoparticles, J. Environ. Health Sci. Eng., 13 (2015) 1–8.

[8] Z. Fang, J. Chen, X. Qiu, X. Qiu, W. Cheng, L. Zhu, Effective removal of antibiotic metronidazole from water by nanoscale zero valent iron particles, Desalination, 268 (2011) 60–67.

[9] M. Noori-Sepehr, T. Al-Musawi, E. Ghahramani, H. Kazemian, M. Zarrabi, Adsorption performance of magnesium/aluminum layered double hydroxide nanoparticles for metronidazole from aqueous solution, Arab. J. Chem., 10 (2016) 611–623.

[10] P.K. Jjemba, The effect of chloroquine, quinacrine and metronidazole on both soybean plants and soil microbiota, Chemosphere, 46 (2002) 1019–1025.

[11] A. Bendesky, D. Menéndez, P. Ostrosky-Wegman, Is metronidazole carcinogenic? Mutat. Res., 511 (2002) 133–144.

[12] IARC, Evaluation of Carcinogenic Risk to Humans. International Agency for Research on Cancer, Lyon, France, 1987, pp. 250–251.

[13] J. Rivera-Utrilla, G. Prados Joya, M. Sánchez-Polo, M.A. Ferro, I. Bautista-Toledo, Removal of nitroimidazole antibiotics from aqueous solution by adsorption/desorption on activated carbon, J. Hazard. Mater., 170 (2009) 298–305.

[14] S.L. Nolasco-Gómez, G. Roa-Morales, R.M. Gómez-Espinosa, P. Balderas-Hernández, P. Ibarra-Millán, Degradation of metronidazole in aqueous solution by electrochemical peroxidation, J. Electrochem. Soc., 1 (2013) 25–33.

[15] I. Ali, M. Asim, T. Khan, Low cost adsorbents for the removal of organic pollutants from wastewater, J. Environ. Manage., 113 (2012) 170–183.

[16] T. Salem, X. Lin, D. Quiang, Synthesized magnetic nanoparticles coated zeolitic for the adsorption of pharmaceutical compounds from aqueous solution using batch and column studies, Chemosphere, 93 (2013) 2076–2085.

[17] W. Shaobin, P. Yuelian, Natural zeolites as effective adsorbents in water and wastewater treatment, Chem. Eng. J., 156 (2010) 11–24.

[18] G.V. Tsitsishvili, T.G. Andronikashvili, G.N. Kirov, L.D. Filizova, Natural Zeolites, Ellis Horwood Limited, Great Britain, 1992.

[19] C. Perego, R. Bagatin, M. Tagliabue, R. Vignola, Zeolites and related mesoporous materials for multi-talented environmental solutions, Microporous Mesoporous Mater., 166 (2013) 37–49.

[20] J. Xie, W. Meng, D. Wu, Z. Zhang, H. Kong, Removal of organic pollutants by surfactant modified zeolite: comparison between ionizable phenolic compounds and non-ionizable organic compounds, J. Hazard. Mater., 231–232 (2012) 57– 63.

[21] G.M. Haggerty, R.S. Bowman, Sorption of chromate and other inorganic anions by organo-zeolitic, Environ. Sci. Technol., 28 (1994) 452–458.

[22] K. Barczyk, W. Mozgawa, M. Król, Studies of anions sorption on natural zeolites, Spectrochim. Acta, Part A, 133 (2014) 876–882.

[23] R. Cortés-Martínez, M. Solache-Ríos, V. Martínez-Miranda, R. Alfaro-Cuevas, Removal of cadmium by natural and surfactant-modified Mexican zeolitic rocks in fixed bed columns, Water, Air, Soil Pollut., 196 (2009) 199–210.

[24] Y. Dong, D. Wu, X. Chen, Y. Lin. Adsorption of bisphenol A from water by surfactant-modified zeolitic, J. Colloid Interface Sci., 348 (2010) 585–590.

[25] D. Krajišnik, A. Daković, A. Milojević, M. Malenović, M. Kragović, D. Bajuk-Bogdanović, V. Dondur, J. Milić, Properties of diclofenac sodium sorption onto natural zeolite modified with cetylpyridinium chloride, Colloids Surf., B, 83 (2011) 165–172.

[26] V. Rakic, N. Rajic, N. Davorik, A. Auroux, The adsorption of salicylic acid, acetylsalicylic acid and atenolol from aqueous solutions onto natural zeolites and clays: clinoptilolite, bentonite and kaolin, Microporous Mesoporous Mater., 166 (2013) 185–194.

[27] C.B. Vidal, G.S.C. Raulino, A. Barros, C.A. Lima, J.P. Ribeiro, M.J.R. Pires, R.F. Nascimento, BTEX removal from aqueous solutions by HDTMA-modified Y zeolite, J. Environ. Manage., 112 (2012) 178–185.

[28] R. Leyva-Ramos, N.A. Medellín-Castillo, R.M. Guerrero-Coronado, M.S. Berber Mendoza, A. Aragón Piña, A. Jacobo Azuara, Intercambio iónico de plata (I) en solución acuosa sobre clinoptilolita, Rev. Int. Contam. Ambient., 21 (2005) 193–200.

[29] Z. Li, R.S. Bowman, Counterion effects on the sorption of cationic surfactant and chromate on natural clinoptilolite, Environ. Sci. Technol., 31 (1997) 2407–2412.

[30] P.A. Gamboa, J.J. Ramírez-García, M. Solache-Ríos, M.C. Díaz-Nava, J.L. Gallegos-Pérez, Comparison of different modified aluminosilicate networks for the removal diclofenac, Desal. Wat. Treat., 57 (2016) 26401–26413.

[31] M. Dávila-Estrada, J.J. Ramírez-García, M.C. Díaz Nava, M. Solache-Ríos, Sorption of 17α-ethinylestradiol by surfactant-modified zeolite-rich tuff from aqueous solutions, Water, Air, Soil Pollut., 227 (2016) 157.

[32] USP (United States Pharmacopeia) 40/National Formulary (NF) 35, Food and Drug Administration (FDA), USA, 2017.

[33] ICH Q2A, Validation of Analytical Procedures: Text and Methodology, European Medicine Agency Web, 2009, Available at: http://www.ema.europa.eu/docs/en_GB/document_library/Scientific_guideline/2009/09/WC500002662.pdf, Accessed 20 June 2017.

[34] ICH Q2B, Validation of Analytical Procedures, European Medicine Agency Web, 2009, Available at: http://www.ema.europa.eu/docs/en_GB/document_library/Scientific_guideline/2009/09/WC500002662.pdf, Accessed 20 June 2017.

[35] FEUM (Farmacopea de los Estados Unidos Mexicanos), Secretaria de Salud, México, 2014.

[36] Y. Yanev, N. Popov, T. Iliev, T. Popova, Zeolitized pyroclastic rocks from Oaxaca (southern Mexico): mineralogy, ion-exchange properties, and use, Geo Chem. Miner. Petrol., 45 (2007) 29–38.

[37] P. Cappelletti, A. Conella, A. Langella, M. Mercurio, L. Catalanotti, V. Monetti, B. de Gennaro, Use of Surface modified natural zeolite (SMNZ) in pharmaceutical preparations Part 1. Mineralogical and technological characterization of some industrial zeolite rich-rocks, Microporous Mesoporous Mater., 250 (2015) 232–244.

[38] B.d. Gennaro, L. Catalanotti, R.S. Bowman, M. Mercurio, Anion exchange selectivity of surfactant modified clinoptilolite-rich tuff for environmental remediation, J. Colloid Interface Sci., 430 (2014) 178–183.

[39] G. Salinas, F. Becerril, M. Solache-Ríos, M.T. Olguín, C. Fall, Determinación de la capacidad de intercambio catiónico (CIC) de zeolita natural del Estado de Oaxaca, México, Memorias del Segundo Congreso Mexicano de Zeolitas Naturales, 2001, pp. 44–48.

[40] F. Mumton, C. Ormsby, Morphology of zeolites in sedimentary rocks by scanning electron microscopy, Clays Clay Miner., 24 (1976) 1–23.

[41] M.C. Díaz-Nava, M.T. Olguín, M. Solache-Ríos, M.T. Alarcón-Herrera, A. Aguilar-Elguezabal, Characterization and improvement of ion exchange capacities of Mexican clinoptilolite-rich tuffs, J. Inclusion Phenom. Macrocyclic Chem., 51 (2005) 231–240.

[42] C. Colella, Environmental Applications of Natural Zeolitic Materials Based on their Ion Exchange Properties, Springer Science, Switzerland AG, 1999, pp. 207–224.

[43] S. Jevtić, S. Grujić, J. Hrenović, N. Rajić, Surfactant modified clinoptilolite as a salicylate carrier, salicylate kinetic release and its antibacterial activity, Microporous Mesoporous Mater., 159 (2012) 30–35.

[44] W. Mozgawa, M. Król, T. Bajda, IR spectra in the studies of anion sorption on natural sorbents, J. Mol. Struct., 993 (2011) 109–114.

[45] E. Katsou, S. Malamis, M. Tzanoudaki, K.J. Haralambous, M. Loizidou, Regeneration of natural zeolitic polluted by lead and zinc in wastewater treatment systems, J. Hazard. Mater., 189 (2011) 773–786.

[46] Y.S. Ho, G. McKay, Sorption of dyes and copper ions onto biosorbents, Process Biochem., 38 (2003) 1047–1061.

[47] H. Ding, G. Bian, Adsorption of metronidazole in aqueous solution by Fe-modified sepiolite, Desal. Wat. Treat., 55 (2015) 1620–1628.

[48] P. Liu, Q. Wang, C. Zheng, C. He, Sorption of sulfadiazine, norfloxacin, metronidazole, and tetracycline by granular activated carbon: kinetics, mechanisms, and isotherms, Water, Air, Soil Pollut., 228 (2017) 129.

[49] L. Sun, D. Chen, S. Wan, Z. Yu, Adsorption studies of dimetridazole and metronidazole onto biochar derived from sugarcane bagasse: kinetic, equilibrium, and mechanisms, J. Polym. Environ., 26 (2018) 765–777002E.

[50] S.V. Manjunath, S.M. Kumar, H.H. Ngo, W. Guo, Metronidazole removal in powder-activated carbon and concrete-containing graphene adsorption systems: estimation of kinetic, equilibrium and thermodynamic parameters and optimization of adsorption by a central composite design, J. Environ. Sci. Health, Part A, 52 (2017) 1269–1283.

[51] E.M. Kalhori, T.J. Al-Musawi, E. Ghahramani, H. Kazemian, M. Zarrabi, Enhancement of the adsorption capacity of the light-weight expanded clay aggregate surface for the metronidazole antibiotic by coating with MgO nanoparticles: studies on the kinetic, isotherm, and effects of environmental parameters, Chemosphere, 175 (2017) 8–20.

[52] F. Polesel, K. Lehnberg, W. Dott, S. Trapp, K.V. Thomas, B.G. Plósz, Factors influencing sorption of ciprofloxacin onto activated sludge: experimental assessment and modelling implications, Chemosphere, 119 (2015) 105–111.

[53] R.E. Huddleston, Surface-Altered Hydrophobic Zeolites as Sorbents for Hazardous Organic Compounds, Institute of Mining and Technology, New Mexico, 1990.

[54] D. Neel, Quantification of BTX Sorption to Surface-Altered Zeolites; Hydrology Open File Report No. H92-2, New Mexico Institute of Mining and Technology, Socorro, NM, 1992.

[55] M.C. Díaz-Nava, M.T. Olguín, M. Solache-Ríos, Adsorption of phenol onto surfactants modified bentonite, J. Inclusion Phenom. Macrocyclic Chem., 74 (2012) 67–75.

[56] M.C. Díaz-Nava, M.T. Olguín, M. Solache-Ríos, M.T. Alarcón Herrera, A. Aguilar Elguezabal, Phenol sorption on surfactant-modified Mexican zeolitic-rich tuff in batch and continuous systems, J. Hazard. Mater., 167 (2009) 1063–1069.

[57] M. Solache-Ríos, M.T. Olguín, I. García-Sosa, J. Jiménez-Becerril, Evaluation of the sorption properties of a Mexican organo clinoptilolite-rich tuff for phenol and 4-chlorophenol, Environ. Technol., 25 (2004) 819–824.

[58] M.G. Vázquez Mejía, M. Solache-Ríos, V. Martínez-Miranda, Removal of fluoride and arsenate ions from aqueous solutions and natural water by modified natural materials, Desal. Wat. Treat., 85 (2017) 271–281.

[59] V. Vimonses, S. Lei, B. Jin, C. Chow, C. Saint, Kinetic study and equilibrium isotherm analysis of Congo Red adsorption by clay materials, Chem. Eng. J., 148 (2009) 354–364.